Chapter 6

Fluorescence from doubly driven four-level system - A density matrix approach

6.1 Introduction

In the previous chapter we described the experimental observation of narrow fluorescence from doubly driven atoms. In this chapter we examine theoretically, using the density matrix formalism, the various processes that occur when 4-level atoms are subject to two driving fields.

The state of a system can be described by the density operator ρ, which is defined by $\rho = |\psi\rangle\langle\psi|$, where $|\psi\rangle$ is the state function. The density operator can be written in terms of n×n density matrix, where n is the number of state functions that completely spans the Hilbert space. In general, the state function can be expanded in a basis set $|\phi_n\rangle$ as $|\psi\rangle = \sum_{i=1}^{n} c_i|\phi_i\rangle$. So that the elements of the density matrix becomes $\rho_{ij} = \langle\phi_i|\rho|\phi_j\rangle = \langle\phi_i|\psi\rangle\langle\psi|\phi_j\rangle = c_i c_j^*$. The normalization of the state function yields $T_r(\rho) = \langle\psi|\psi\rangle = 1$

In the case of a two level atom, n=2, and therefore ρ is a 2×2 matrix. The elements ρ_{ij} depend on the basis states $|\phi_n\rangle$. The diagonal element $|c_i|^2$ is the probability for the atom to be in state i, which takes a value between 0 and 1. The off diagonal elements $c_i c_j^*$ are called the coherence since they depend upon the phase difference between c_i and c_j.

In general for a two level system the state function can be written as

$$|\psi\rangle = c_1 e^{(i\xi_1)}|1\rangle + c_2 e^{(i\xi_2)}|2\rangle \tag{6.1}$$

where c_1 and c_2 are real.

If $\xi_1 - \xi_2$ is constant coherence exists. If ξ_1 and ξ_2 are random then for a collection of two level systems $\langle e^{i(\xi_1-\xi_2)}\rangle = 0$, and $\rho_{ij} = 0$ (for $i \neq j$), and thus the density matrix becomes diagonal. If the system goes to a coherent state entire system is defined by a density matrix

$$\rho = \begin{vmatrix} |c_1|^2 & c_1c_2^* \\ c_2c_1^* & |c_2|^2 \end{vmatrix}$$

Diagonal elements satisfy the condition $|c_1|^2 + |c_2|^2 = 1$

We have considered ^{85}Rb atoms as a four level system and therefore, ρ is a 4×4 matrix. The initial treatments in literature of alkali elements have been as a two-level system, with a ground and excited state. This gives rise to the Rabi oscillations under the action of an external field ([1]). However, the existence of fine structure and the D1 and D2 lines show that a more accurate picture of an alkali element would be in terms of a three-level system. Numerous treatments of three level systems exist in the literature ([2] to [5]). These may be classified as **Λ, V,** Ξ (ladder) systems as shown in figure 6.1. These give rise to a variety of phenomena like electro-magnetically induced transparency (EIT), lasing without inversion (LWI) etc.

The hyperfine splitting of the levels clearly indicates that a three level system too is a simplification. Therefore, four level systems have been studied ([6] - [8]). Our treatment, however, differs from these in that we have considered ^{85}Rb as an inverted N system and have also consider the motion of the atoms in co- and counter-propagating geometries with

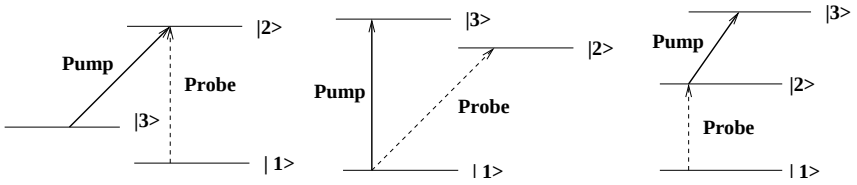

Figure 6.1: Λ, V, and Ξ systems.

respect to the cooling and repumper beams.

6.2 The Four Level Density Matrix

The four levels under consideration are the two ground hyperfine levels $5S_{1/2}$ F = 2, 3 and the two excited levels $5P_{3/2}$ $F' = 3', 4'$ (see fig.6.2a). For simplicity, we have considered an

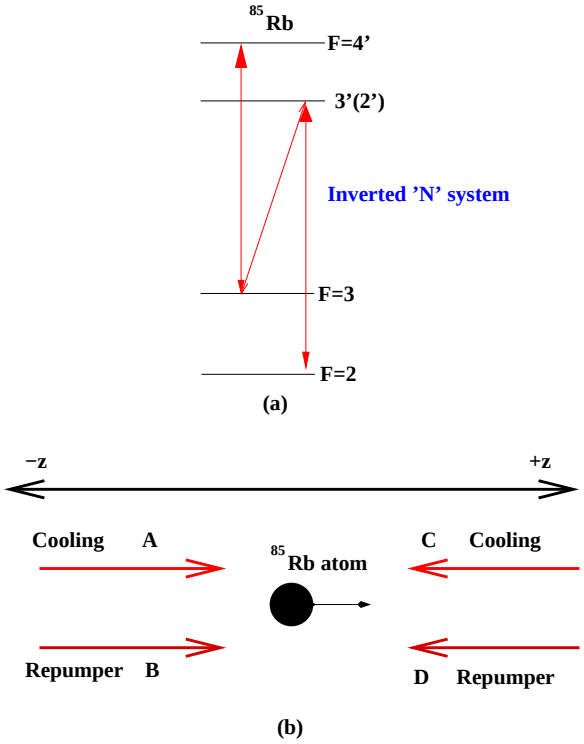

Figure 6.2: (a) Four energy levels of our system (b): An one dimensional configuration(along z) of the cooling and repumper beams with the ^{85}Rb atom taken moving along the +z direction.

one dimensional situation where the two driving laser fields are in the $\pm z$ direction and the atom is moving along the +z direction with a velocity **v** (figure 6.2b). The detuning of the cooling laser is δ_c in the laboratory frame. In the frame of the moving atom, the detuning Δ_c $= \delta_c - \mathbf{k_c} \cdot \mathbf{v}$ for an atom approaching the cooling beam. If one were to consider the transition

from F = 3 − >F′ = 3, the detuning $\Delta_{c3'} = 121 + \delta_c - \mathbf{k_c} \cdot \mathbf{v}$, where 121 MHz is the separation of the F′ = 3 level from the F′= 4 level [1].

Similarly, for the repumper, detuning $\Delta_r = \delta_r - \mathbf{k_r} \cdot \mathbf{v}$ where δ_r is the detunings of the repumper laser in the laboratory frame, and $\mathbf{k_r}$ is the wavevector of the repumper beam. Since the frequencies of the cooling and repumper beams differ only by a few GHz we may take $k_r = k_c$. The total Hamiltonian for the system consisting of a stationary atom and the light fields is written in the interaction picture as

$$H = H_0 + H_I \tag{6.2}$$

where H_0 is the Hamiltonian for the bare atom and H_I is the atom-light interaction Hamiltonian. They are given as

$$H_0 = \hbar\omega_2|2><2| + \hbar\omega_3|3><3| + \hbar\omega_{3'}|3'><3'| + \hbar\omega_{4'}|4'><4'| \tag{6.3}$$

and

$$\begin{aligned} H_I = -\frac{\hbar}{2}[&\Omega_{34'}|3><4'|\exp(-i\omega_{LC}t) + \Omega_{33'}|3><3'|exp(-i\omega_{LC}t) \\ &+\Omega_{23'}\exp(-i\omega_{LR}t)|2><3'| + H.C] \end{aligned} \tag{6.4}$$

Here the $\hbar\omega_i$ represent the energies of the levels as represented in figure 6.2, with $\hbar\omega_2$ taken as zero, ω_{LC} and ω_{LR} the frequencies of the cooling and repumper laser beams and $\Omega_{ij'}$ is the Rabi frequency connecting the levels i and j'. The total Hamiltonian can be written in matrix form as follows

$$H = \begin{vmatrix} \hbar\omega_2 & 0 & -\frac{\hbar}{2}\Omega_{23'}e^{(-i\omega_{LR}t)} & 0 \\ 0 & \hbar\omega_3 & -\frac{\hbar}{2}\Omega_{33'}e^{(-i\omega_{LC}t)} & -\frac{\hbar}{2}\Omega_{34'}e^{(-i\omega_{LC}t)} \\ -\frac{\hbar}{2}\Omega_{23'}e^{(i\omega_{LR}t)} & -\frac{\hbar}{2}\Omega_{33'}e^{(i\omega_{LC}t)} & \hbar\omega_{3'} & 0 \\ 0 & -\frac{\hbar}{2}\Omega_{34'}e^{(i\omega_{LC}t)} & 0 & \hbar\omega_{4'} \end{vmatrix}$$

where the rows and columns correspond to levels $2, 3, 3', 4'$ in sequence. The cooling laser beam can cause transitions $3 - > 4'$ and $3 - > 3'$. As the dipole moment matrix elements for the two transitions are different $\Omega_{34'}$ is different for the same beam from $\Omega_{33'}$. The dynamics

[1] levels of $5P_{3/2}$ are denoted primed

of the system described by this Hamiltonian can be studied using the density matrix $\rho = \sum \rho_{ij}|i><j|$. The time evolution of the density matrix ρ is given by the Liouville equation

$$\frac{d\rho}{dt} = -\frac{i}{\hbar}[H,\rho] - \frac{1}{2}\{\Gamma,\rho\} \tag{6.5}$$

where [A, B] is a commutator and {A,B} is an anti-commutator, with

$$\Gamma_{ij} = 2\gamma_{i\rightarrow j'}\delta_{ij'} \tag{6.6}$$

where the second term of the equation (6.5) is the spontaneous decay term. $\gamma_{i\rightarrow j'}$ is half the spontaneous decay rate from the j'^{th} level to the i^{th} level. The decay rate from $4'$(due to the spontaneous transition $4'->3$) is $2\gamma_{4'3}$ and from $3'$ (due to the spontaneous transition $3'->3$, $3'->2$) are $\gamma_{3'3}$ and $\gamma_{3'2}$ i.e.

$$\Gamma_{4'4'} = 2\gamma_{4'3} \tag{6.7}$$

$$\Gamma_{3'3'} = 2\gamma_{3'3} + 2\gamma_{3'2} \tag{6.8}$$

$$\Gamma_{33} = -2\gamma_{4'3} - 2\gamma_{3'3} \tag{6.9}$$

$$\Gamma_{22} = -2\gamma_{3'2} \tag{6.10}$$

Γ_{ij} is diagonal.

The rate equations of the four levels for an atom moving with a velocity v are derived under the Rotating Wave Approximation (i.e. suitably choosing a rotating frame to eliminate the rapid time variation in $\rho_{ij}(t)$). They are

$$\frac{d\rho_{22}}{dt} = -\frac{i}{2}[\Omega_{23'}\rho_{3'2} - \Omega^*_{23'}\rho_{23'}] + 2\gamma_{3'2}\rho_{33'} \tag{6.11}$$

$$\frac{d\rho_{23}}{dt} = -i(\Delta_{c3'} - \Delta_r)\rho_{23} - \frac{i}{2}[\Omega_{23'}\rho_{3'3} - \Omega^*_{33'}\rho_{23'} - \Omega^*_{34'}\rho_{24'}] \tag{6.12}$$

$$\frac{d\rho_{23'}}{dt} = (i(\Delta_r) - (\gamma_{3'2} + \gamma_{3'3}))\rho_{23'} - \frac{i}{2}[\Omega_{23'}\rho_{3'3'} - \Omega^*_{23'}\rho_{22} - \Omega^*_{33}\rho_{23}] \tag{6.13}$$

$$\frac{d\rho_{24'}}{dt} = -i[(\Delta_{c3'} - \Delta_c - \Delta_r) - i\gamma_{4'3}]\rho_{24'} - \frac{i}{2}[\Omega_{23'}\rho 34' - \Omega_{34'}\rho_{23}] \tag{6.14}$$

$$\frac{d\rho_{32}}{dt} = i(\Delta_{c3'} - \Delta_r)\rho_{32} - \frac{i}{2}[\Omega_{33'}\rho_{3'2} + \Omega_{34'}\rho_{4'2} - \Omega_{23'}\rho_{33'}] \tag{6.15}$$

$$\frac{d\rho_{33}}{dt} = -\frac{i}{2}[\Omega_{33'}\rho_{3'3} + \Omega_{34'}\rho_{4'3} - \Omega_{33'}\rho_{33'} - \Omega_{34'}\rho_{34'}]$$
$$+ 2\gamma_{3'3}\rho_{3'3'} + 2\gamma_{4'3}\rho_{4'4'} \tag{6.16}$$

$$\frac{d\rho_{33'}}{dt} = (i\Delta_{c3'} - (\gamma_{3'2} + \gamma_{3'3}))\rho_{33'} - \frac{i}{2}[\Omega_{33'}\rho_{3'3'} + \Omega_{34'}\rho_{4'3'} - \Omega_{23'}\rho_{32} - \Omega_{33'}\rho_{33}] \quad (6.17)$$

$$\frac{d\rho_{34'}}{dt} = (i\Delta_c - \gamma_{4'3})\rho_{34'} - \frac{i}{2}[\Omega_{33'}\rho_{3'4'} + \Omega_{34'}\rho_{4'4'} - \Omega_{34'}\rho_{33}] \quad (6.18)$$

$$\frac{d\rho_{3'2}}{dt} = (-i\Delta_r - (\gamma_{3'2} + \gamma_{3'3}))\rho_{3'2} - \frac{i}{2}[\Omega^*_{23'}\rho_{22} + \Omega^*_{33'}\rho_{32} - \Omega^*_{23'}\rho_{3'3'}] \quad (6.19)$$

$$\frac{d\rho_{3'3}}{dt} = (-i\Delta_{c3'} - (\gamma_{3'2} + \gamma_{3'3}))\rho_{3'3} - \frac{i}{2}[\Omega^*_{23'}\rho_{23} + \Omega^*_{33'}\rho_{33} - \Omega^*_{33}\rho_{3'3'} - \Omega_{34'}\rho_{3'4'}] \quad (6.20)$$

$$\frac{d\rho_{3'3'}}{dt} = -2(\gamma_{3'2} + \gamma_{3'3})\rho_{3'3'} - \frac{i}{2}[\Omega_{23'}\rho_{23'} + \Omega^*_{33'}\rho_{33'} - \Omega_{33'}\rho_{3'3} - \Omega_{23'}\rho_{3'2}] \quad (6.21)$$

$$\frac{d\rho_{3'4'}}{dt} = [(i\Delta_{c3'} - \Delta_c) - (\gamma_{3'2} + \gamma_{3'3} + \gamma_{4'3})]\rho_{3'4'} - \frac{i}{2}[\Omega^*_{23'}\rho_{24'} + \Omega^*_{33'}\rho_{34'} - \Omega_{34'}\rho_{3'3}] \quad (6.22)$$

$$\frac{d\rho_{4'2}}{dt} = [(i\Delta_{c3'} - \Delta_c - \Delta_r) - \gamma_{4'3}]\rho_{4'2} - \frac{i}{2}[\Omega^*_{34'}\rho_{32} - \Omega^*_{23'}\rho_{4'3'}] \quad (6.23)$$

$$\frac{d\rho_{4'3}}{dt} = [(i\Delta_c - \gamma_{4'3})]\rho_{4'3} - \frac{i}{2}[\Omega^*_{34'}\rho_{33} - \Omega^*_{33'}\rho_{4'3'} - \Omega^*_{34'}\rho_{4'4'}] \quad (6.24)$$

$$\frac{d\rho_{4'3'}}{dt} = [-i(\Delta_{c3'} - \Delta_c) - (\gamma_{3'2} + \gamma_{3'3} + \gamma_{4'3})]\rho_{4'3'} - \frac{i}{2}[\Omega_{34'}\rho_{33'} - \Omega_{33'}\rho_{4'3} - \Omega^*_{23'}\rho_{4'2}] \quad (6.25)$$

$$\frac{d\rho_{4'4'}}{dt} = -\frac{i}{2}[\Omega^*_{34'}\rho_{34'} - \Omega_{34'}\rho_{4'3} - 2\gamma_{4'3}\rho_{4'4'}] \quad (6.26)$$

with the constraint $\rho_{22} + \rho_{33} + \rho_{3'3'} + \rho_{4'4'} = 1$. Therefore, the number of equations to be solved is reduced from 16 to 15 now. In the steady state $d\rho/dt = 0$, and the 15 equations can be written in the form

$$M\rho + \varphi = 0 \quad (6.27)$$

$$\Rightarrow \rho = -M^{-1}\varphi \quad (6.28)$$

where M is a 15x15 square matrix, ρ is a 15x1 column matrix, and φ is also a 15x1 column matrix. Therefore, to obtain the steady-state values of elements of ρ, the matrix M has to be inverted and the product of M^{-1} and -φ to be taken.

Calculations were done taking typical values of parameters $\Omega_{23'} = 0.3$ MHz, $\Omega_{34'} = 6.0$ MHz, $\Omega_{33'} = 5.0$ MHz, $\gamma_{4'3} = 6.0$ MHz, $\gamma_{3'3} = 2.6$ MHz, $\gamma_{2'3}$= 2.07 MHz, which approximately corresponds to our experimental situation. For each velocity **v** steady state values of

ρ_{ij} are obtained by numerically solving the above rate equations for various values of δ_c and δ_r. Thus for an atom with a velocity **v** we obtain the population of each level and coherence between various levels for different values of δ_r and δ_c. The fluorescence emitted (due to the transitions of the atom from the excited state) by the atom with a velocity **v** is given by

$$\text{Fluorescence}(\Delta_c, \Delta_r) = \Gamma_{4'3}\rho_{4'4'} + \Gamma_{3'3}\rho_{3'3'} + \Gamma_{3'2}\rho_{3'3'} \tag{6.29}$$

As the detector collects fluorescence from atoms in a thermal ensemble, we take the ρ_{ij} value over the range of velocities, weighted by the one dimensional Maxwellian velocity distribution.

$$\text{Fluorescence}(\delta_c, \delta_r) = < \text{Fluorescence}(\Delta_c, \Delta_r) >_v \tag{6.30}$$

The four level scheme in figure 6.2 considers the repumping transition 2 - >3′. However, the transition 2 − >2′ also serves to repump atoms to the cooling cycle. The entire calculation was therefore repeated, this time for levels 2,3,2′, 4′. In this case $\Delta_{c3'}$ is replaced by $\Delta_{c2'} = \delta_c$ + 183 MHz. The two results were then combined. A representative result is presented with the corresponding experimental data, in figure 6.3 for a cooling laser detuning $\delta_c = -162$ MHz. A general agreement between the results of our calculation and that of the experiment is seen. The individual features will be discussed in detail now.

6.3 Discussion

Consider a situation shown in figure (6.2)b, when both the cooling and repumping beams are along ± z directions. Initially let us consider the atoms to be at rest. For a given detuning δ_c of the cooling (pump) laser, we should get fluorescence peaks corresponding to the Autler-Townes (AT) dressed states of $F' = 3'$ at the probe (repumper) detunings [9]

$$\delta_{r\pm} = \frac{\delta_{c3'}}{2} \pm \sqrt{(\delta_{c3'}^2 + \Omega^2)}/2 \tag{6.31}$$

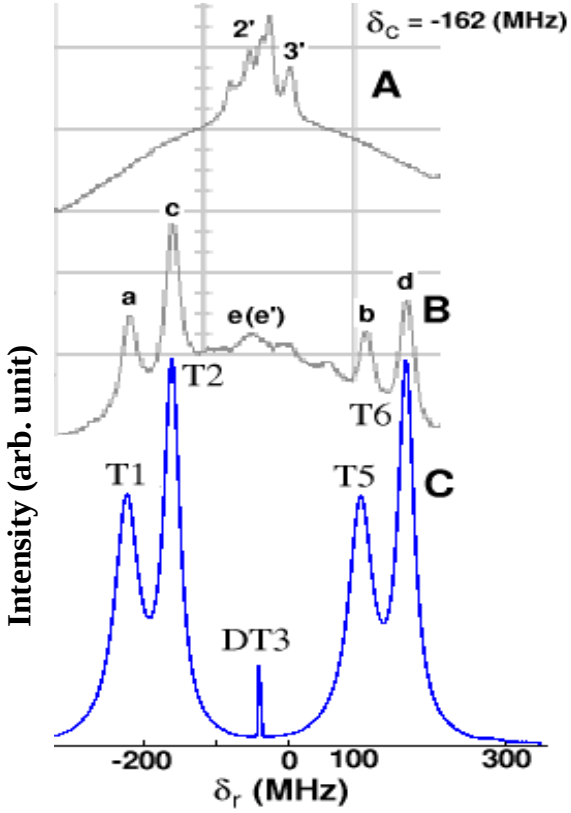

Figure 6.3: Trace A shows the saturation absorption spectrum of the repumper the frequency of which is scanned in time. Trace B gives the experimentally observed fluorescence. The a, b, c, d, e(e') labels represent the peak positions as found in the experiment. Trace C shows the results of the density matrix calculations for the same δ_c taking the levels F = 2, 3 and F′ = 3′(2′) and 4′ into account. The T1,T2, DT3, T5 and T6 labels the resultant theoretically derived peak positions.

Here $\delta_{c3'}$ = 121 MHz + δ_c denotes the detuning of the cooling laser from 3 → 3′ transition, 121 MHz being the level spacing between F′ = 3′ and 4′ levels and Ω its Rabi frequency. These peaks arise due to the dynamic Stark splitting of level F′ = 3′. In general, a level with total angular momentum J will split into J+1 levels. Thus the $5S_{1/2}$ state with J = 0 is not split; the $5P_{3/2}$, with J=1 splits into two levels. Transitions from the unsplit ground state to each of the split upper level gives rise to two peaks at $\delta_{r\pm}$. The widths of the peaks vary as

$$\Gamma_{\pm} = \frac{\Gamma}{2}\left(1 \mp \frac{\delta_{c3'}}{\sqrt{\delta_{c3'}^2 + \Omega^2}}\right) \tag{6.32}$$

The equations (6.31) and (6.32) show both the positions and widths of the peaks depend

upon $\delta_{c3'}$. $\delta_{c3'} = 0$ makes them symmetric and widths same which is half the unperturbed width Γ. Any non-zero value of $\delta_{c3'}$ reduces the width of one peak further while the other one gets broadend proportionally such that total widths of the two peaks becomes exactly equal to their unperturbed width Γ. The specific case shown in fig.6.3, for a cooling laser detuning δ_c = -162 MHz and for small Ω, the Autler-Townes peak positions for zero velocity atoms are $\delta^0_{r\pm} \approx$ -41 and 0 MHz respectively. The population of levels F = 2 and F′= 3 (ie ρ_{22} and $\rho_{3'3'}$) are shown in figure 6.4a for stationary atoms. Figure 6.4b gives the absorption (Im ($\rho 23'$) due to the transition $2 - > 3'$, that shows the AT doublet.

From figure 6.4a which gives the populations in levels F = 2 and F = 3, we see that the occurrence of F = 3 peaks at precisely the frequency at which F = 2 gets depopulated, indicating a transfer of population from F = 2 to F = 3.

Let us now consider an atom in motion (figure 6.2b). If $\delta_c < 0$ this atom predominantly absorbs from the cooling beam C coming towards it. This causes AT splitting of the F′ = 3′ level of this atom. Since the repumper laser is scanned, depending on the sign of δ_r the atom absorbs either from B or from D. Thus absorption of repumper will occur at four different detunings of a given δ_c of the cooling laser. The same holds for $\delta_c > 0$ for atoms with velocity $-v$.

The AT doublet positions at which absorption will occur in a frame where the atom is at rest (atom frame) are 0 and (121 + (δ_c + kv)). However, from the laboratory frame these positions will get Doppler shifted to

$$\delta_{r-} = \delta^0_{r-} - kv \approx -kv; \quad \delta_{r+} = \delta^0_{r+} - kv \approx \delta_{c3'} = 121 + \delta_c \tag{6.33}$$

when the repumper light is absorbed from D (see figure 6.2)

$$\delta_{r-} = \delta^0_{r-} + kv \approx +kv; \quad \delta_{r+} = \delta^0_{r+} + kv \approx \delta_{c3'} + 2kv \tag{6.34}$$

when the repumper light is absorbed from B.

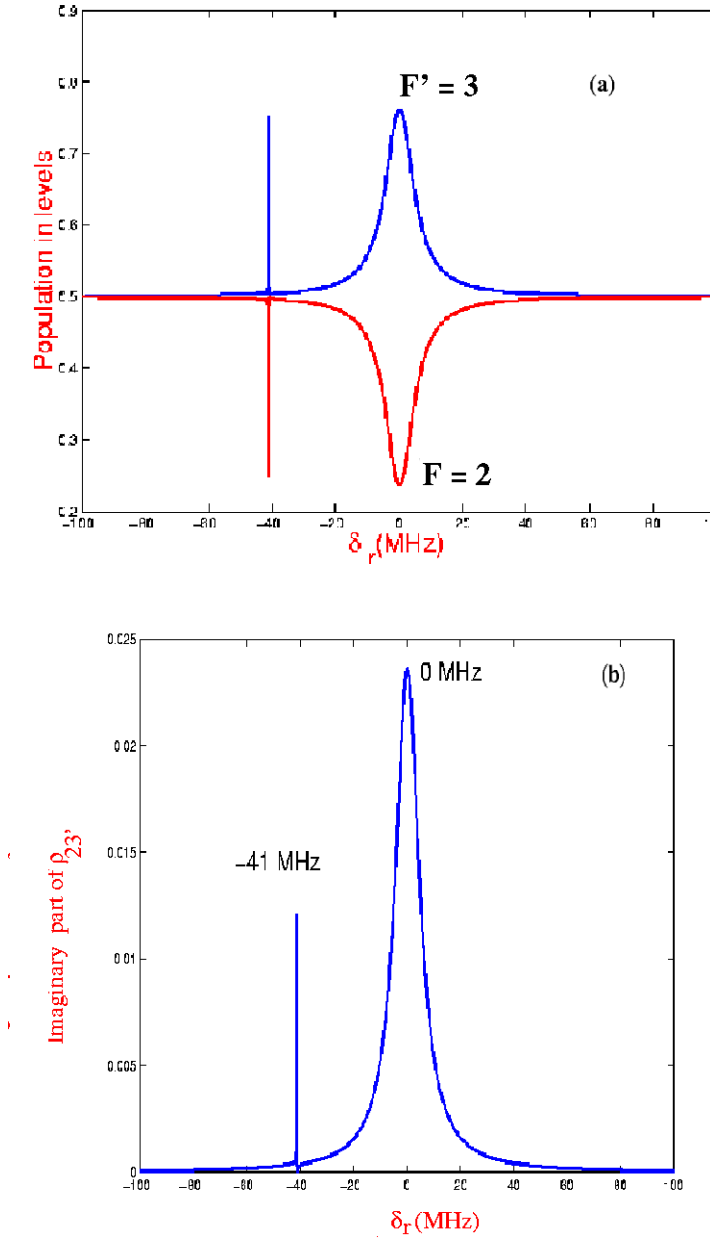

Figure 6.4: (a)The population in levels F = 2 and F = 3 ρ_{33}, ρ_{22} respectively as functions of δ_r. (b) The imaginary part of $\rho_{23'}$ vs the repumper (probe) laser frequency δ_r showing that absorption of the repumper (probe) light due to Autler -Townes splitting of the level F′ = 3′ occurs at the detunings 0 MHz and -41 MHz.

A simple way to understand this is as follows. We have to apply the suitable detuning to the laser so that atom absorbs the photons. Depending upon the direction of the velocity of the atom and that of the photon we have to choose the suitable detuning. As the atom is moving in the +z direction, if it has to absorb the repumper photon from beam D, then the beam should have red detuning. When absorbption is from B, then blue detuning is needed. The same holds for $\delta_c > 0$.

The gas contains Rb atoms with a Maxwellian distribution of velocity. Not all atoms can participate in fluorescence, as the Doppler shift will cause most of the atoms to find the lasers out of resonance. In fact, only a small velocity class around v_c which satisfies the relation

$$v_c = |\delta_c|/k \tag{6.35}$$

will give rise to fluorescence. This is the mechanism that gives rise to narrow velocity selection from a hot gas. This velocity selection effect is confirmed by our calculations and is shown in figure 6.5 which gives $\rho_{4'4'}$ and $\rho_{3'3'}$ as functions of the velocity of the atom for $\delta_c = \delta_r$= -162 MHz.

We see that the population in F′ = 4′ ($\rho_{4'4'}$) is two orders more than that in F′ = 3′ ($\rho_{3'3'}$) and it peaks at the critical velocity v_c = 126 m/sec. Therefore, only for atoms with velocities around v_c both the repumper and the cooling laser become resonant to the corresponding transitions, showing that indeed the ($\mathbf{k} \cdot \mathbf{v} = \delta_c$) resonance condition selects a narrow velocity class for fluorescence from a thermal ensemble with a Doppler width ≈ 2 GHz.

Using the resonance condition, we get the position of the AT peaks

$$\delta_{r-} = \delta_c; \quad \delta_{r+} = 121 \text{ MHz} + \delta_c \tag{6.36}$$

when absorption takes place from D (see figure 2) and

$$\delta_{r-} = -\delta_c; \quad \delta_{r+} = 121 \text{ MHz} - \delta_c(v = v_c) \tag{6.37}$$

$$\delta_{r+} = 121 \text{ MHz} + \delta_c + 2kv(v \neq v_c) \tag{6.38}$$

when the repumper absorption takes place from B.

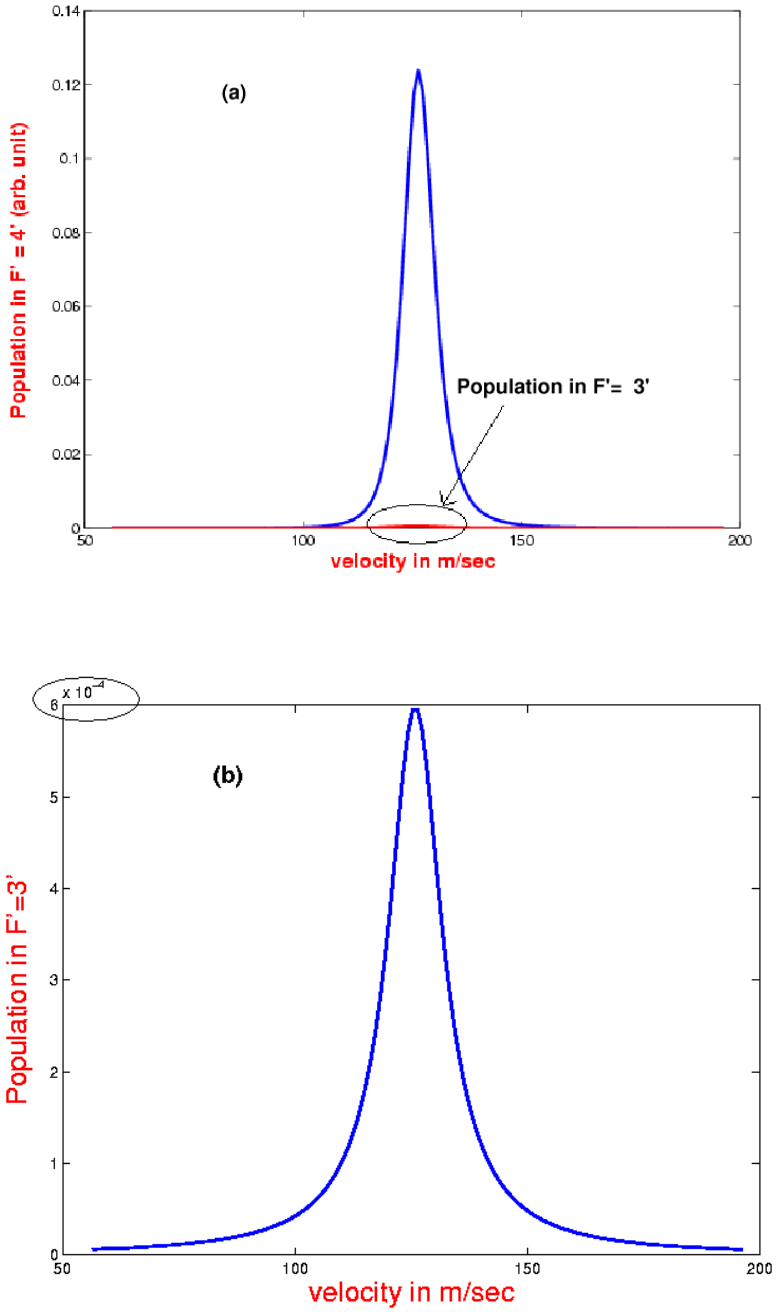

Figure 6.5: (a) Populations in the upper levels F′ = 4′ and F′ = 3′. (b) Zoom-in of the population in F′ = 3′ (Note reduced y axis scale in (b).)

These peak positions, given δ_c = -162 MHz will occur for repumper detunings at -162 MHz(T2), -41 MHz(DT3), +162 MHz(T6) (see fig. 6.3) and 283 MHz. We see that experimentally we get all expected peaks within the range of our repumper scan. The same peak positions are obtained for atoms with a velocity $-v$, for $\delta_c > 0$.

It has been estimated in [10] that the peak at δ_{r-} is broad and the one at δ_{r+} is narrow. The height of the AT peaks decide the prominence of a fluorescence peak as it decides the number of atoms participating in the fluorescence. Thus for peak positions $\delta_{r-} = \delta_c$ & $-\delta_c$ we expect a large fluorescence whereas for the peak at $\delta_{r+} = 121$ MHz$+\delta_c$ we expect a much smaller fluorescence as is indeed seen from experiment and from our calculations (fig.6.3).

The peak at 283MHz around $\delta_{r+} = 121$ MHz + $\delta_c + 2kv$ is absent both in experiment and in our density matrix calculation. For this case, the repumper absorption takes place from B whereas the cooling is absorbed from C. When the absorption takes place from counter-propagating cooling and repumper beams the velocity class satisfying the double resonance is severely restricted. In fact only for $v = v_c$ will the double resonance condition be satisfied. Atoms with $v \neq v_c$ will see the cooling and repumper to be shifted by opposite detunings and hence will not contribute to the fluorescence. Thus the peak resulting from this configuration will not be seen as only a very small number of atoms contribute to it. The severely restricted velocity range at resonance resulting in the absence of the peak at 121 MHz + δ_c + 2kv is illustrated in figure6.6b which is obtained from the density matrix calculation. As we see here, only a small number in a very narrow velocity range contribute to population in $F' = 4'$ in contrast to the case $\delta_{r-} = -\delta_c$ (fig.6.6a).

The peaks marked T1, DT3 and T5 in figure 6.3 are the peaks corresponding to the AT levels of $F' = 2'$ due to absorption from counter and co propagating repumper beams. These peaks can be obtained from the same four-level density matrix calculation by replacing the level $F' = 3'$ by $F' = 2'$. Thus the peaks are obtained at

$$\delta_{r-} = \pm\delta_c = \pm 162 \text{ MHz} \tag{6.39}$$

$$\delta_{r+} = (184 \text{ MHz} + \delta_c) = +22 \text{ MHz} \tag{6.40}$$

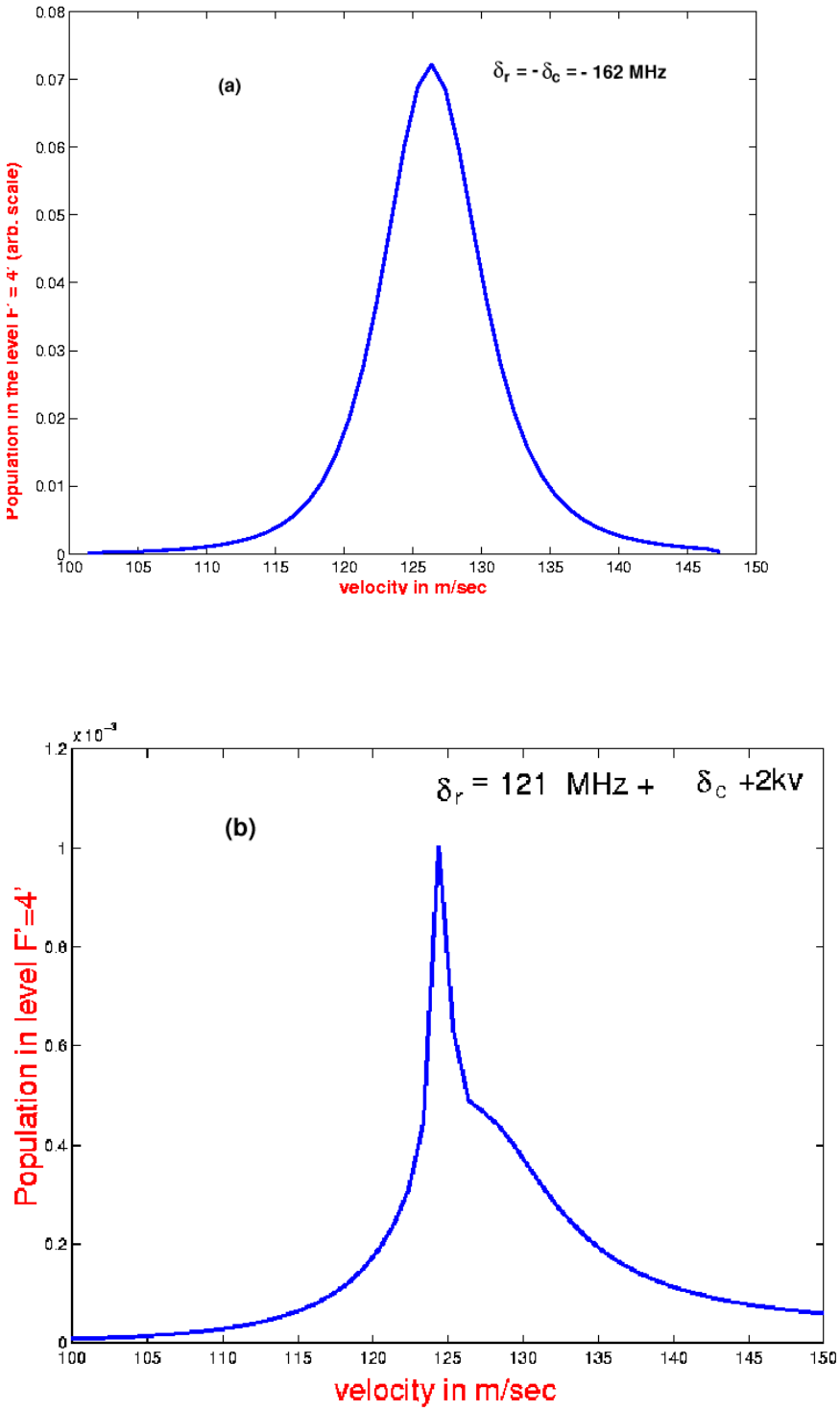

Figure 6.6: Population in the level F′ = 4′ as a function of the velocity of atoms for the Autler-Townes peaks at (a) $\delta_r = -\delta_c = 162$ MHz (b) $\delta_r = 121$ MHz + δ_c +2kv (Note reduced y- axis scale in (b)).

with 184 MHz being the hyperfine separation between $F' = 4'$ and $F' = 2'$ level. Here the detuning δ_c is measured from the $F' = 2'$ transition. But in the experimental scan we measured separations from $F' = 3'$ transitions. This gives rise to peaks T1 and T5 and another peak at the position of DT3 peak of $F' = 3'$ transition (see figure6.3). It is seen that the peak positions of T1 and T5 can be simply obtained from the corresponding peaks for $F' = 3'$ by shifting them by - 63 MHz, this being the hyperfine separation between $F' = 3'$ and $F' = 2'$. The theoretically calculated widths of the fluorescence peaks match with the experimentally observed narrow width of about 30 MHz. It should be emphasised that this does not arise due to the cooling of atoms in the optical molasses like configuration but due to the existence of a velocity selection as discussed before. These fluorescence peaks are experimentally seen to be narrow even for blue detunings of the cooling beam where no cooling occurs and the atoms are at room temperature. The expected Doppler width at this temperature is nearly 2 GHz.

6.4 Conclusions

Existence of narrow fluorescence peaks in the absence of induced coherence in a doubly driven multi-level atomic system has been explained using a four-level density matrix formalism. The theory finds that the fluorescence peaks are given rise by the Autler-Townes (AT) splitting of $F' = 3'$ and $F' = 2'$ levels for atoms around a particular velocity class. The AT splitting is seen to occur due to the strong cooling laser and hence is dependent on its detuning δ_c. The repumper which connects $F' = 3'$ and $F' = 2'$ to F = 2 pumps the atoms from F = 2 to F = 3. The cooling laser connects F = 3 to $F' = 4'$ and causes fluorescence. Because the repumper becomes efficient in pumping atoms from 2 -> 3 for the velocity class of atoms satisfying the double resonance condition the fluorescence shows a narrow peak at double resonance. The theory accounts for all the peaks seen in the experiment and also explains the experimental absence of the other two peaks. The widths of the peaks agree quite well with the experimentally obtained widths.

Bibliography

[1] " Quantum Optics" by Marlan O. Scully and M. Suhail, Zubairy, Cambridge University press, United Kingdom, (1997).

[2] S. E. Harris, Physics Today **50**, 36(1997) and references therein; A.S. Zibrov, et al., Physical Review Letters **75**, 1499(1995); E. Arimondo, Progress in Optics, edited by E. Wolf (Elsevier, Amsterdam, 1996), vol. XXXV.

[3] S.N. Sandhya, K. K. Sharma, Physical Review A **55**, 2155 (1997).

[4] C. Wei , D. Suter, A. S. M. Windsor and Neil B. Manson, Physical Review A **58**, 2310 (1998).

[5] S. R. de Echaniz, D. Andrew. Greentree, A. V. Durrant, D.M. Segal, J. P. Marangos, and J. A. Vaccaro, Physical Review A **64**, 013812(2001).

[6] M.D. Lukin, S.F. Yelin, M. Fleischhauer, M. O. Scully, Physical Review A **60**, 3225 (1999).

[7] Y. Abranyos, M. Jacob, and J. Bergou, Physical Review A **60**, R2618(1999).

[8] C. Y. Ye, A.S. Zibrov, Yu. V. Rostovtsev, M.O.Scully, Physical Review A **65**, 043805 (2002).

[9] G. Vemuri, G. S. Agarwal, B.D. Nageswara Rao, Physical Review A **53**, 2842(1996).

[10] G. S. Agarwal, Physical Review A **54**, 3734(1996).